Computational Mechanics 21 (1998) 477–482 © Springer-Verlag 1998

Mixed mode fatigue growth of curved cracks emanating from fastener holes in aircraft lap joints

J. H. Park, S. N. Atluri

Abstract The finite element alternating method is extended further for analyzing multiple arbitrarily curved cracks in an isotropic plate under plane stress loading. The required analytical solution for an arbitrarily curved crack in an infinite isotropic plate is obtained by solving the integral equations formulated by Cheung and Chen (1987a, b).

With the proposed method several example problems are solved in order to check the accuracy and efficiency of the method. Curved cracks emanating from loaded fastener holes, due to mixed mode fatigue crack growth, are also analyzed. Uniform far field plane stress loading on the plate and sinusoidally distributed pin loading on the fastener hole periphery are assumed to be applied. Small cracks emanating from fastener holes are assumed as initial cracks, and the subsequent fatigue crack growth behavior is examined until long arbitrarily curved cracks are formed near the fastener holes under mixed mode loading conditions.

1 Introduction

The finite element alternating method (FEAM) has been known to be an effective method for obtaining accurate stress intensity factors. The method has been applied successfully to two dimensional cracks as well as three dimensional cracks (Atluri 1986, 1997). However, until now, in the case of plane problems, the method was limited to the case of multiple arbitrarily oriented straight line cracks. In this paper the FEAM is extended further in order to analyze multiple curved cracks in a finite isotropic plate under plane stress. With the newly proposed method, we can obtain SIF values for general multiple curved cracks, and also can simulate fatigue crack growth of multiple curved cracks in plane sheets under mixed mode loading conditions.

In the FEAM, an analytical solution for a curved crack in an infinite isotropic plate under plane stress is required. The required solution is obtained here by solving the integral equations formulated by Cheung and Chen (1987a, b, 1993). In this formulation, cracks are modeled as continuous distributions of dislocations. Integral equations can be derived, under the given tractions or resultant forces on crack surfaces, for the unknown dislocation density function. Cheung and Chen (1987a, b, 1993) showed that several types of integral equations, such as Cauchy singular, weakly singular or hypersingular integral equations, can be derived. In this paper we use the weakly singular integral equations, because of the convenience in manipulating the integrals (Zang and Gudmundson 1991). After solving for the dislocation density functions, stress intensity factors and stress fields can be calculated.

In order to check the accuracy and efficiency of the proposed method several example problems are solved and compared with the previously published results. Curved cracks emanating from loaded fastener holes in plane stress sheets, representative of aircraft lap joints, are also analyzed. Uniform far field plane stress loading on the plate and sinusoidally distributed pin loading on the fastener hole periphery are assumed to be applied. Small hole cracks are assumed as initial cracks, and fatigue crack growth behavior is examined until long curved cracks are formed near the fastener holes under mixed mode loading conditions.

From several sample problems presented here, we conclude that the FEAM is as convenient a method for analyzing curved cracks as previously found for analyzing straight cracks. Since the crack configuration can be chosen independently of the FEM mesh, the remeshing procedure is not necessary during the arbitrarily curved growth of cracks in a fatigue analysis. So FEAM can be used conveniently in arbitrarily curved crack growth simulation. Indeed, in the simulation of arbitrarily curved crack growth, the FEAM is more convient than the Element Free Galerkin Methods (Belytschko et al. 1994).

2 Formulation

Consider the problem of a curved through-thickness crack embedded in an infinite isotropic plate under plane stress/strain conditions. Arbitrary surface tractions are assumed to be applied on the crack surface. In order to obtain the proper stress functions for the problem, we treat the curved crack as a distribution of dislocations.

Communicated by G. Yagawa, 12 November 1997

S. N. Atluri
Center for Aerospace Research & Education
7704, Boelter Hall, School of Engineering & Applied Science,
UCLA Los Angeles, CA, 90095-1600 USA

J. H. Park
Dept. of Safety Engng, Chungbuk National University,
Cheongju, Chungbuk 361–763, Rep. of Korea

Correspondence to: J. H. Park

The support of FAA, and the encouragement of C. C. Seher are thankfully acknowledged. The first author is partly supported by KOSEF (KOSEF 961-1004-033-2).

The complex stress functions for a dislocation located at $z = z_0$ are given as (Santare and Keer 1986):

$$\phi(z) = \gamma \log(z - z_0) \ ,$$
$$\psi(z) = \bar{\gamma} \log(z - z_0) - \gamma \frac{\overline{z_0}}{z - z_0} \ , \tag{1}$$

where $\gamma = G(b_x + ib_y)/i\pi(\kappa + 1)$, G is shear modulus and $\kappa = 3 - 4\nu$ for plane strain and $\kappa = (3 - \nu)/(1 + \nu)$ for plane stress, here ν is Poisson's ratio. Also b_x and b_y are the Cartesian components of the Burgers vector. The relations between the stresses and the complex stress functions are given as (Muskhelishvili 1953):

$$\sigma_x + \sigma_y = 2\left[\phi'(z) + \overline{\phi'(z)}\right] \ ,$$
$$\sigma_y - \sigma_x + 2i\tau_{xy} = 2[\bar{z}\phi''(z) + \psi'(z)] \ . \tag{2}$$

The resultant force X and Y acting on an arc AB are expressed as (Muskhelishvili 1953):

$$X + iY = -i\left[\phi(z) + z\overline{\phi'(z)} + \overline{\psi(z)}\right] + c_1 \ , \tag{3}$$

where the point A is a fixed point on the given arc, and the point B is an arbitrary point on the arc. z denotes the coordinate of the point B, and c_1 is a complex constant.

From Eq. (1) the stress functions for a distribution of dislocations along an arc L can be expressed as follows [3]:

$$\phi(z) = \int_L D(s) \log(z - t)\, \mathrm{d}s \ ,$$
$$\psi(z) = \int_L \overline{D(s)} \log(z - t)\, \mathrm{d}s - \int_L \frac{\bar{t} D(s)}{(z - t)}\, \mathrm{d}s \ . \tag{4}$$

Where,

$$D(s) = D_1(s) + iD_2(s) = \frac{G\left[B_x(s) + iB_y(s)\right]}{i\pi(\kappa + 1)} \ . \tag{5}$$

Here s is the distance from a fixed point to a point t along the arc; and $B_x(s)$ and $B_y(s)$ are the x and y components of the dislocation density function at s on the arc. Substituting Eq. (4) into Eq. (3) and letting z approach the point t_0 on the arc, we can obtain:

$$i[X(t_0) + iY(t_0)] = \int_L 2 \log|t - t_0| D(s)\, \mathrm{d}s + \int_L \frac{t - t_0}{\bar{t} - \bar{t}_0} \overline{D(s)}\, \mathrm{d}s + c_1 \ . \tag{6}$$

By letting $t - t_0 = r(t, t_0) \exp[i\theta(t, t_0)]$, we can obtain the following integral equations from Eq. (6), as in Cheung and Chen (1987b):

$$\int_L 2 \log[r(t, t_0)] D_1(s)\, \mathrm{d}s + \int_L \big\{ D_1(s) \cos[2\theta(t, t_0)] + D_2(s) \sin[2\theta(t, t_0)] \big\}\, \mathrm{d}s + \mathrm{Re}(c_1) = -Y(t_0)$$
$$\int_L 2 \log[r(t, t_0)] D_2(s)\, \mathrm{d}s + \int_L \big\{ D_1(s) \sin[2\theta(t, t_0)] - D_2(s) \cos[2\theta(t, t_0)] \big\}\, \mathrm{d}s + \mathrm{Im}(c_1) = X(t_0) \tag{7}$$

In addition, in order to satisfy the single valuedness of displacements, we have:

$$\int_L D_i(s)\, \mathrm{d}s = 0 \quad (i = 1, 2) \ . \tag{8}$$

In order to solve the Eqs. (7) and (8), the curved crack L is divided into n line segments $L_1, L_2, \ldots, L_n$ and also each line segment is assumed to be straight. Let the end points of the kth line segment be t_k and t_{k+1}. Also we assume that the dislocation density value at an internal point of each line segment can be expressed in terms of the values at the end points by using suitable interpolation functions. Since the dislocation density function has a $1/\sqrt{r}$ singularity at the crack tips, we can assume the dislocation density functions as follows. For the first and the last line segments,

$$D_i(\xi) = \sqrt{\frac{2}{1 + \xi}} \left[\frac{1 - \xi}{2} (D_i)_1 + \frac{1 + \xi}{2} (D_i)_2 \right] \quad (i = 1, 2) \tag{9}$$

$$D_i(\xi) = \sqrt{\frac{2}{1 - \xi}} \left[\frac{1 - \xi}{2} (D_i)_n + \frac{1 + \xi}{2} (D_i)_{n+1} \right] \quad (i = 1, 2) \tag{10}$$

And for the kth line segment excluding the first and the last segments,

$$D_i(\xi) = \frac{1 - \xi}{2} (D_i)_k + \frac{1 + \xi}{2} (D_i)_{k+1} \quad (i = 1, 2) \tag{11}$$

Here ξ is the local coordinate in each line segment, and $-1 \le \xi \le 1$. $(D_i)_k$ represents the dislocation density function value at the kth point ($k \neq 1$, $k \neq n + 1$). Dislocation distributions assumed here are the same as those used by Zang and Gudmundson (1991) for kinked cracks.

After substituting Eqs. (9), (10) and (11) into Eqs. (7) and (8) and integrating each terms for $t_0 = t_k$ ($k = 1, \ldots, n + 1$), we can obtain $(2n + 4)$ simultaneous algebraic equations for $(2n + 4)$ unknowns. The unknowns are D_1 and D_2 values at t_k ($k = 1, \ldots, n + 1$) and real and imaginary part of c_1.

During the integration for each term of integral equations, the following integrals are evaluated in closed form. For the next integral:

$$I_k = \int_{L_k} 2 \log[r(t, t_0)] D_i(s)\, \mathrm{d}s \tag{12}$$

the integration values are as follows:

$$I_1 = \frac{4l_1}{9} \left[2(3 \log l_1 - 8)(D_i)_1 + (3 \log l_1 - 2)(D_i)_2 \right] \quad (\text{when } t_0 = t_1)$$
$$I_1 = \frac{4l_1}{9} \left[2(3 \log l_1 + 6 \log 2 - 5)(D_i)_1 + (3 \log l_1 + 6 \log 2 - 8)(D_i)_2 \right] \quad (\text{when } t_0 = t_2)$$
$$I_n = \frac{4l_n}{9} \left[(3 \log l_n + 6 \log 2 - 8)(D_i)_n + 2(3 \log l_n + 6 \log 2 - 5)(D_i)_{n+1} \right] \quad (\text{when } t_0 = t_n)$$
$$I_n = \frac{4l_n}{9} \left[(3 \log l_n - 2)(D_i)_n + 2(3 \log l_n - 8)(D_i)_{n+1} \right] \quad (\text{when } t_0 = t_{n+1}) \tag{13}$$

If k is not equal to 1 or n,

$$I_k = l_k\left[\left(\log l_k - \frac{3}{2}\right)(D_i)_k + \left(\log l_k - \frac{1}{2}\right)(D_i)_{k+1}\right] \quad (\text{when } t_0 = t_k) \tag{14}$$

$$I_k = l_k\left[\left(\log l_k - \frac{1}{2}\right)(D_i)_k + \left(\log l_k - \frac{3}{2}\right)(D_i)_{k+1}\right] \quad (\text{when } t_0 = t_{k+1})$$

Here l_k is the length of the kth line segment. Also for the next integral:

$$J_k = \int_{L_k} D_i(s)\,\mathrm{d}s \tag{15}$$

the integration values are:

$$\begin{aligned} J_1 &= \frac{2}{3} l_1\left[2(D_i)_1 + (D_i)_2\right] \\ J_n &= \frac{2}{3} l_n\left[(D_i)_n + 2(D_i)_{n+1}\right] \\ J_k &= \frac{1}{2} l_k\left[(D_i)_k + (D_i)_{k+1}\right] \quad (k \neq 1,\ k \neq n) \end{aligned} \tag{16}$$

Other integral values are obtained from numerical integration. Suitable Gaussian type integration formulas are used in the presence of $1/\sqrt{t}$ type singularity (Abramowith and Stegun 1972).

Once $(D_i)_1$ and $(D_i)_{n+1}$ are known at the crack tips, the stress intensity factors can be calculated from the following relations:

$$\begin{aligned} K_{\mathrm{I}} &= (2\pi)^{3/2}\sqrt{l}\left[(D_1)_c \cos\alpha + (D_2)_c \sin\alpha\right] \ , \\ K_{\mathrm{II}} &= (2\pi)^{3/2}\sqrt{l}\left[(D_1)_c \sin\alpha - (D_2)_c \cos\alpha\right] \ . \end{aligned} \tag{17}$$

Here l is the length of the line segment which includes crack tip. So l can be l_1 or l_n. And α is the angle determined as follows. Let t_c be crack tip point and t_a be the other end point in the corresponding line segment. So t_c can be t_1 or t_{n+1} and t_a can be t_2 or t_n. α is the argument of $t_c - t_a$, so $t_c - t_a = l\exp(i\alpha)$. And the subscript c denotes the values at crack tip.

3
Finite element alternating method

A general and detailed description of the finite element alternating method can be found in Atluri (1986, 1997). The basic steps in the FEAM for curved cracks are the same as the usual FEAM for straight cracks. The basic steps are described here briefly.

(1) Using the finite element method, to model only the uncracked sheet, obtain the stresses at the locations of the cracks in a finite sheet subjected to given boundary tractions and/or pin loading on fastener hole peripheries. Here cracks are not included in the FEM model, but the fastener holes are included in the FEM model, when we consider cracks near fastener holes.
(2) To create the traction free crack surfaces, erase the stresses on the crack surfaces, that are computed in Step (1), using the analytical solution for a curved crack given in section 2 in this paper. Determine the SIF at each of the crack tips. Note that the resultant forces, instead of tractions, are used in the formulation for analytical solutions. Here, numerical integration is carried out along the crack to obtain resultant forces from the tractions obtained at Gaussian integration points.
(3) Corresponding to the solutions in Step (2), determine the residual tractions at the surfaces of all the fastener holes as well as the outer boundaries of the finite body. For the case of multiple curved cracks, obtain the residual traction on each crack surface, caused by the presence of the other cracks.
(4) In order to satisfy the given traction boundary conditions at the outer boundaries of the finite sheet as well as at the surfaces of all the fastener holes, reverse the residual tractions at these surfaces. Using the finite element method, calculate the equivalent nordal forces at the finite element nodes on these surfaces.
(5) Using the finite element method to obtain the stresses at the location of the cracks corresponding to the nodal forces as calculated in Step (4).
(6) Add the residual stresses on the crack surfaces obtained from Step (3) from the other cracks, and from Step (5). Erase the residual stresses on crack surfaces by repeating Step (2).
(7) Continue the iteration until the increments in SIF resulting from Step (6) are vanishingly small.
(8) By summing all the appropriate contributions, compute the total SIF for each of the tips of each the curved cracks.

4
Arbitrarily curved crack growth near loaded fastener holes

With the proposed method, arbitrarily curved crack growth near loaded fastener holes under fatigue loading is analyzed. For calculating fatigue crack growth increment, Forman's equation is used. Forman's equation is given by (Forman et al. 1967):

$$\frac{\mathrm{d}a}{\mathrm{d}N} = \frac{C(\Delta K)^n}{(1-R)K_c - \Delta K} \ . \tag{18}$$

Here ΔK is the stress intensity factor range and R is the stress ratio in cyclic loading. In this paper, the material is assumed to be 2024-T3 aluminium alloy. In this case the values of $K_c = 83\,000\ \mathrm{psi}\sqrt{\mathrm{in}}$ $(91.2\ \mathrm{MPa}\sqrt{\mathrm{m}})$, $C = 3 \times 10^{-13}$ and $n = 3$ are used. Here, the unit of crack length is inches and that of SIF is $\mathrm{psi}\sqrt{\mathrm{in}}$. When the units are meter and $\mathrm{MPa}\sqrt{\mathrm{m}}$, $C = 6.3 \times 10^{-9}$ and $n = 3$. And the stress ratio is assumed to be 0.1 in fatigue calculation.

Crack growth direction is determined by using the maximum principal stress criterion (Erdogan and Sih 1963). Crack extension angle θ_m is determined from the following equation:

$$K_{\mathrm{I}} \sin\theta_m + K_{\mathrm{II}}(3\cos\theta_m - 1) = 0 \ . \tag{19}$$

In calculating ΔK in Eq. (18), we use the equivalent stress intensity factor which is defined by:

$$(K_I)_{eq} = K_I \cos^3\frac{\theta_m}{2} - 3K_{II}\cos^2\frac{\theta_m}{2}\sin\frac{\theta_m}{2} \quad . \tag{20}$$

5
Sample problems and discussions

First in order to check the accuracy of the present numerical solution for a curved through-thickness crack in an infinite plane stress sheet, the stress intensity factors of a parabolic crack are obtained and compared with Chen's results (Chen 1993). The crack shape is represented by:

$$y = \alpha(a^2 - x^2)/a \quad |x| < a$$

and shown in Fig. 1. The results are given in Fig. 2. Each normalized stress intensity factor is obtained from the following relations:

$$\begin{aligned} K_{IB} &= F_{IB}(\alpha)\sigma_x^\infty\sqrt{\pi a}, \quad K_{IIB} = F_{IIB}(\alpha)\sigma_x^\infty\sqrt{\pi a}, \\ K_{IB} &= G_{IB}(\alpha)\sigma_y^\infty\sqrt{\pi a}, \quad K_{IIB} = G_{IIB}(\alpha)\sigma_y^\infty\sqrt{\pi a}, \\ K_{IB} &= H_{IB}(\alpha)\sigma_{xy}^\infty\sqrt{\pi a}, \quad K_{IIB} = H_{IIB}(\alpha)\sigma_{xy}^\infty\sqrt{\pi a} \quad . \end{aligned} \tag{21}$$

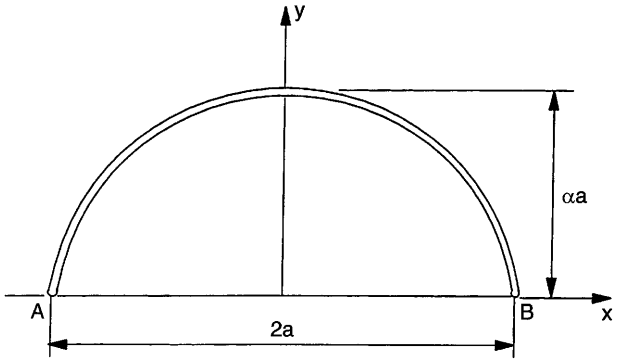

Fig. 1. A parabolic through-thickness crack in a sheet loaded in plane stress

From Fig. 2, we can notice that the present results agree well with those of Chen (1993).

Next straight line cracks emanating from a fastener hole are considered and the calculated mode I SIF values are compared with those of Cartwright and Parker (1982). A circular hole of radius R is assumed to be located at the center of a rectangular plate of width $2W$, height $2H$. Two radial cracks of equal length $(a - R)$ are assumed to emanate along the x axis from the hole. The sheet is assumed to be subject to uniform normal stress σ_0 on the upper horizontal edge, and sinusoidally distributed pin loading is assumed to exist on the lower half of the fastener hole periphery. We assume $H/W = 2$ and $W/R = 4$. The mode I SIF values K_I of this problem can be obtained from the superposition of two symmetric problems (Park et al. 1992). Let K_{IB} be the SIF when uniform normal stress σ_0 is applied on the upper and lower horizontal edge, and K_{IC} be the SIF when sinusoidally distributed pin loading is applied on the upper and lower harves of the fastener hole periphery. Then $K_I = (K_{IB} + K_{IC})/2$. The present results agree very well with those of Cartwright and Parker (1972).

Next, we examine the fatigue crack growth behavior of cracks emanating from fastener holes. The initial crack configuration is as shown in Fig. 4. The hole radius is R, and crack lengths a_1, a_2, a_3 and a_4 are measured from the hole surface. θ_1 is the angle between the x axis and the axis formed by cracks of lengths a_1 and a_2; likewise θ_2 is the angle between the x axis and the axis formed by cracks of lengths a_3 and a_4.

Fig. 5 shows the case when uniform stress $\sigma_0 = 82.74$ MPa (12 ksi) is applied on the upper horizontal edge, $\sigma_0/3$ on the lower horizontal edge, and sinusoidally distributed pin loading is applied on the lower half of the hole periphery. This system of tractions is assumed to be in self-equilibrium. At the initial crack configuration, the mode II SIF is only about 10% of the mode I SIF. So we can find that the kinking angle is small, and that the cracks

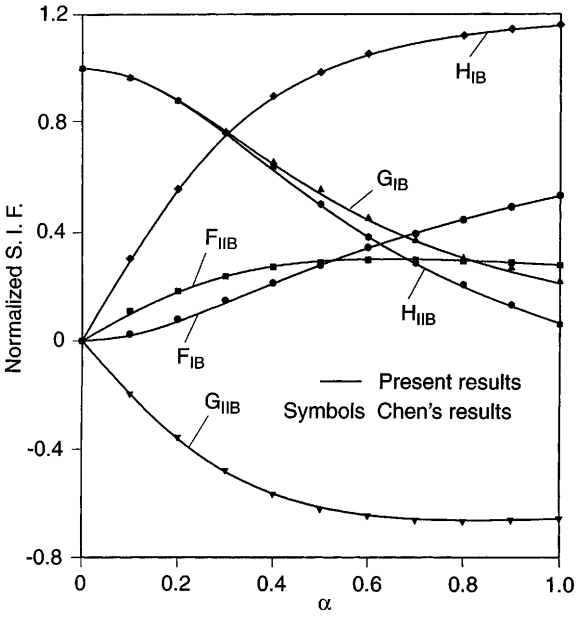

Fig. 2. Normalized S.I.F. for a parabolic through-thickness crack, in a sheet under plane stress

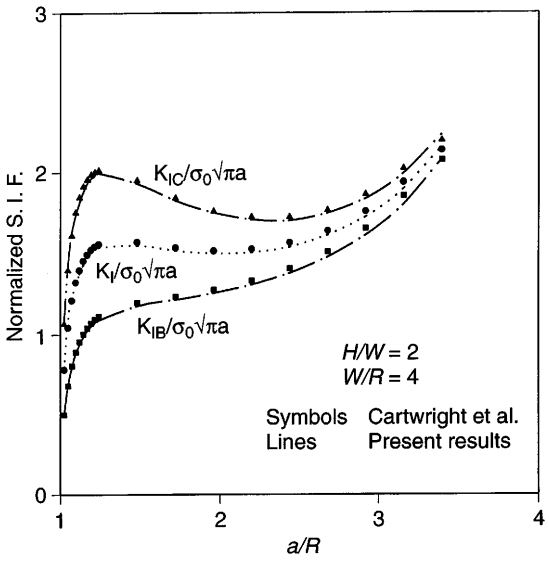

Fig. 3. Variation of normalized S.I.F. as a function of crack length, for a straight line crack along the x axis, emanating from a loaded fastener hole

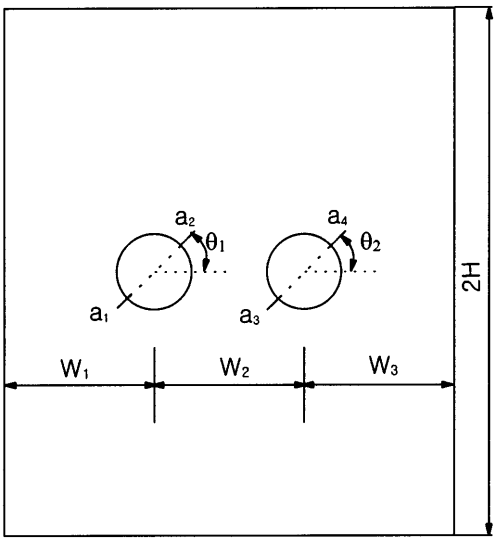

Fig. 4. Assumed initial configurations of cracks emanating from loaded fastener holes

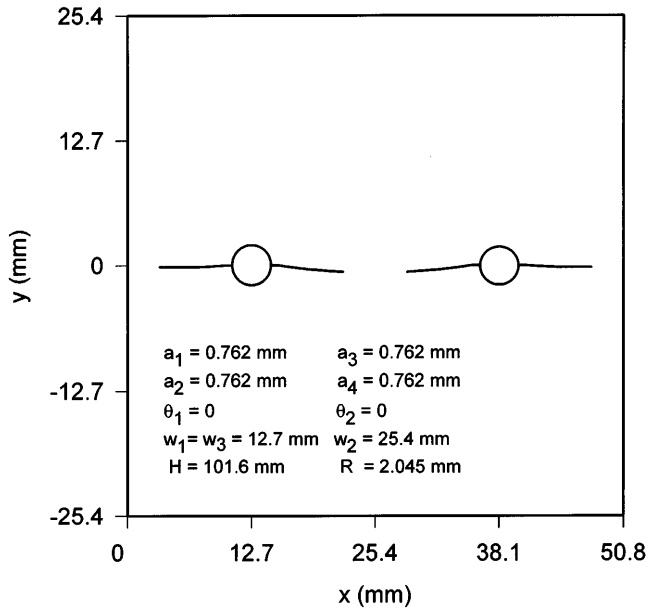

Fig. 5. Fatigue crack growth of cracks near loaded fastener holes. The loading is uniform stress σ_0 on the upper edge of the sheet, $\sigma_0/3$ on the lower edge of the sheet and sinusoidally distributed pin loading on the lower halves of the fastener hole peripheries. The loading system is in self-equilibrium

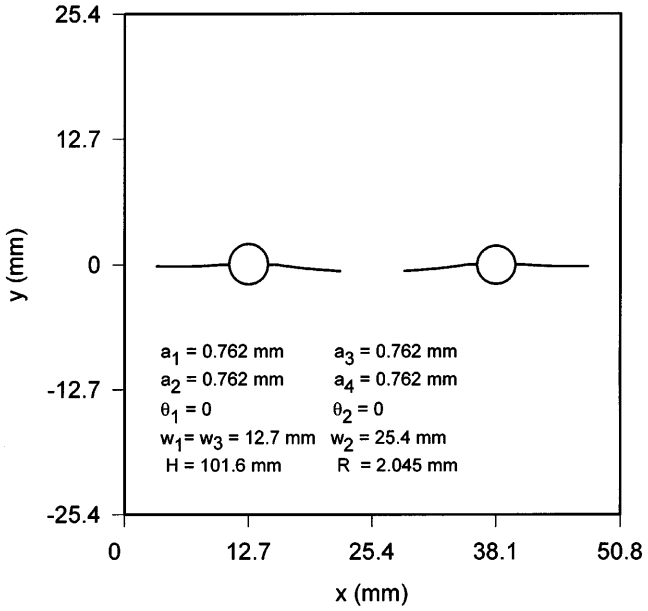

Fig. 6. Fatigue crack growth of cracks near loaded fastener holes. The self-equilibrated loading consists of uniform stress σ_0 on the upper edge of the sheet and sinusoidally distributed pin loadings on the lower halves of the fastener hole peripheries

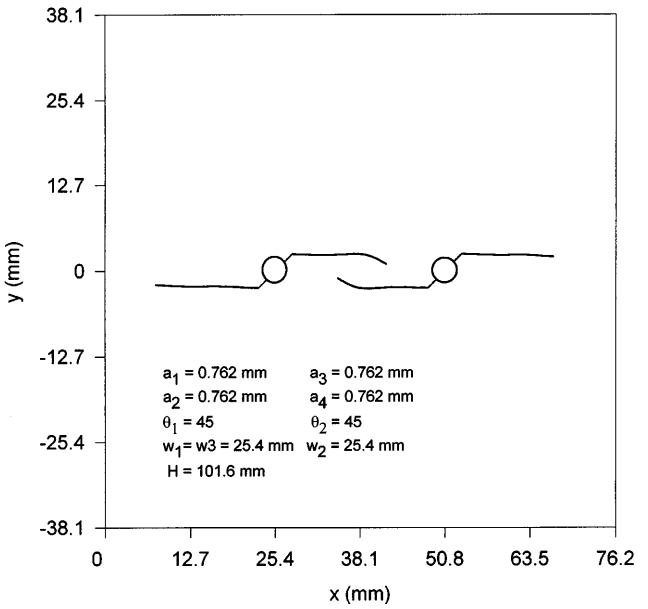

Fig. 7. Fatigue crack growth of hole cracks near fastener holes. The loading consists of uniform stress σ_0 on the upper and lower edges of the sheet

propagate nearly horizontally. Here the total applied loading cycles 26 700 cycles.

Fig. 6 shows the case when uniform stress σ_0 is applied on the upper horizontal edge, and an equilibrating sinusoidally distributed pin loading exists on the lower half of the hole periphery. The crack growth behavior is nearly the same as in Fig. 5. And the total applied loading cycles 19 800 cycles.

Next we assume slanted initial cracks. Fig. 7 is the case when both the initial cracks emanating from the fastener holes are slanted at 45 degrees. Fig. 8 shows the case when the initial cracks emanating from one of the fastener holes are slaned at 20 degrees, and the cracks emanating from the other hole are initially slanted at 0 degree. We can see the fatigue crack growth behavior, involving arbitrarily curved crack growth in the figure.

6 Conclusion

The finite element alternating method is extended further for multiple curved cracks in an isotropic plate. With the

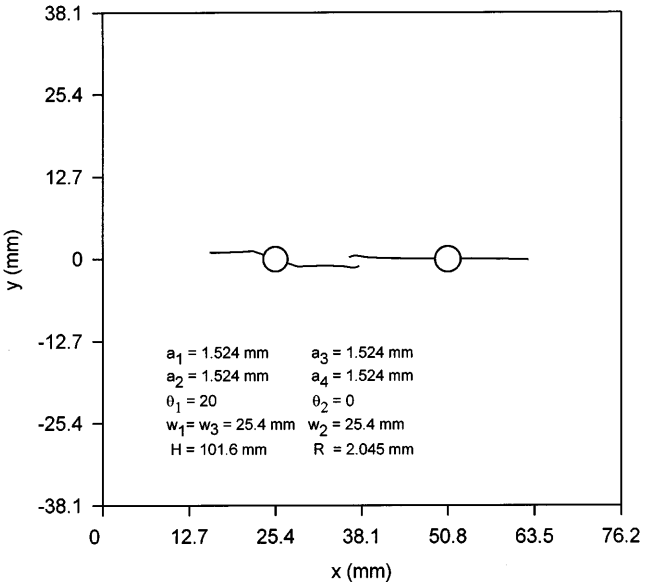

Fig. 8. Fatigue crack growth of hole cracks near fastener holes. The loading consists of uniform stress σ_0 on the upper and lower edges of the sheet

proposed method several example problems are solved in order to check the accuracy and efficiency of the method. Fatigue crack growth behavior is analyzed for curved cracks emanating from loaded fastener holes in sheets, representative of aircraft lap joints. It is found that the proposed method can be used effectively in analyzing general curved cracks and their growth in fatigue.

References

Abramowith M, Stegun IA (1972) Handbook of mathematical functions, Dover, New York

Atluri SN (1986) Computational methods in the mechanics of fracture, North Holland, Amsterdam

Atluri SN (1997) Structural Integrity and Durability, Tech Science Press, Forsyth

Belytschko T, Lu YY, Gu L (1994) Element-free Galerkin methods, Int. J. Num. Meth. in Eng. 37: 229–256

Cartwright DJ, Parker GA (1982) Opening mode stress intensity factors for cracks in pin loads joints, Int. J. Fracture 18: 65–78

Chen YZ (1993) Numerical solution of a curved crack problem by using hypersingular integral equation approach, Eng. Frac. Mech. 46: 275–283

Cheung YK, Chen YZ (1987a) Solutions of branch crack problems in plane elasticity by using a new integral equation approach, Eng. Frac. Mech. 28: 31–41

Cheung YK, Chen YZ (1987b) New integral equation for plane elasticity crack problems. Theoretical and Applied Fracture Mechanics 7: 177–184

Erdogan F, Sih GC (1963) On the crack extension in plates under plane loading and transverse shear, J. Basic Engng 85: 519–527

Forman RG, Kearney VE, Engle RM (1967) Numerical analysis of crack propagation in cyclic-loaded structures, J. Basic. Engng 89: 459–464

Muskhelishvili NI (1953) Some basic problems in the theory of elasticity, Noordhoff, Groningen

Park JH, Ogiso T, Atluri SN (1992) Analysis of cracks in aging aircraft structures, with and without composite-patch repairs, Computational Mechanics 10: 169–201

Santare MH, Keer LM (1986) Interaction between an edge Dislocation and a rigid elliptical inclusion, J. of Appl. Mech. 53: 382–385

Zang WL, Gudmundson P (1991) Kinked cracks in an anisotropic plane modeled by an integral equation method, Int. J. Solids structures 27: 1855–1865